Journal of Magnetism and Magnetic Materials 408 (2016) 193–198

Contents lists available at ScienceDirect

Journal of Magnetism and Magnetic Materials

journal homepage: www.elsevier.com/locate/jmmm

In-plane spin reorientation transition in Co/Py bilayers grown epitaxially on vicinal Cu(001)

J.X. Deng [a,b], A. Tan [b], J. Li [b,c], C. Hwang [d], Z.Q. Qiu [b,*]

[a] College of Electronics and Information, Hangzhou Dianzi University, Hangzhou 310018, PR China
[b] Department of Physics, University of California at Berkeley, Berkeley, CA 94720, USA
[c] International Center for Quantum Materials, Institute of Physics, Peking University, Beijing 100871, PR China
[d] Korea Research Institute of Standards and Science, Yuseong, Daejeon 305-340, Republic of Korea

ARTICLE INFO

Article history:
Received 30 November 2015
Received in revised form
2 February 2016
Accepted 14 February 2016
Available online 19 February 2016

PACS:
75.70.Ak

Keywords:
Magnetic ultrathin films
Magnetic anisotropy
MOKE

ABSTRACT

Co/Py bilayers were grown epitaxially onto a vicinal Cu(001) substrate with the atomic steps parallel to the [110] crystalline axis. We show that the magnetization in vicinal Cu/Co/Py/Cu(001) undergoes an in-plane spin reorientation transition (SRT) from perpendicular to parallel direction of the steps as the Co film thickness increases. By performing Rotation Magneto-Optic Kerr Effect (ROTMOKE) measurement as a function of both the Py and the Co film thicknesses, we show that the observed in-plane SRT results from a competition between the step-induced uniaxial anisotropies in the Py and Co films that favor the Py and Co magnetizations perpendicular and parallel to the atomic steps, respectively. Step decoration experiment further shows that the uniaxial anisotropy originates from the step edges of the vicinal surface.

1. Introduction

Designing and controlling spin axis in a magnetic nanostructure is crucial to the development of spintronics technology. Since the spin direction in a solid is determined by the magnetic anisotropy [1,2,3], the essential issue in controlling the spin orientation is how to manipulate the magnetic anisotropy in a magnetic nanostructure. The two main sources of the magnetic anisotropy are the magnetic dipolar interaction and the spin-orbit interaction [4]. The dipolar interaction depends on the shape of the specimen and is usually responsible for the in-plane magnetization of a magnetic thin film. The spin-orbit interaction depends on the electronic structure and the crystalline symmetry, and thus permits the manipulation of magnetic anisotropy by interface/surface engineering. One representative example is the so-called spin reorientation transition (SRT) [5,6,7] in which the easy magnetization direction changes from perpendicular to in-plane direction of a magnetic thin film. This kind of SRT usually involves the competition between the perpendicular crystalline anisotropy and the in-plane shape anisotropy, and can be controlled by film thickness [8–11], temperature [12,13], structural transformation [5,6], and alloy composition [14], etc. The ability of controlling the perpendicular crystalline magnetic anisotropy has led the discovery of many important and interesting phenomena such as the magnetic stripes [15–17], bubbles [18,19], and the topological magnetic skyrmions [20–22], etc.

Compared with the out-of-plane SRT study, there has been relatively much less effort in controlling the in-plane SRT in magnetic thin films because the dipolar interaction is not involved in the in-plane SRT. The key issue for the in-plane SRT is how to fine tune the in-plane uniaxial magnetic anisotropy. Many different approaches have been developed such as using vicinal surfaces [23,24], off-normal growth [25,26], and piezoelectric substrate [27], etc. aiming to manipulate the in-plane magnetic anisotropy by varying thickness and temperature [28,29]. For example, Welp et al. [30] realized a switching of the magnetization in $Ga_{1-x}Mn_x$ As from [100] (or [010]) to [110] axis as the temperature increases above ½ of the Curie temperature, owing to the interplay between the cubic anisotropy and a uniaxial anisotropy. Li et al. [31] found that Fe/CoO bilayers grown on vicinal MgO(001) could undergo an in-plane SRT by cycling the external magnetic field and attributed this phenomenon to the thermal activation of the CoO domains. Despite the progress made, the control of the in-plane SRT has been more or less limited due to the lack of a fine tune of the in-plane uniaxial magnetic anisotropy.

Recently, Ma et al. investigated Ni/Py bilayers grown on vicinal Cu(001) and found that the atomic steps on vicinal Cu(001) induces an in-plane uniaxial magnetic anisotropy in Py overlayer that favors the Py magnetization perpendicular to the steps and

* Corresponding author.

http://dx.doi.org/10.1016/j.jmmm.2016.02.042
0304-8853/

that the Ni overlayer can further strengthen this step-induced uniaxial anisotropy [32]. Although there is no in-plane SRT in the vicinal Ni/Py/Cu(001), Ma's work demonstrated the capability of fine tuning in-plane uniaxial anisotropy using bilayers on a vicinal surface. Noticing the opposite signs of the step-induced anisotropy in vicinal Co/Cu(001) [33] and the vicinal Py/Cu(001) systems, we carried out a research on Co/Py bilayers grown epitaxially on vicinal Cu(001) substrate. By fabricating the Co/Py bilayers into double cross wedges, we are able to fine tune the step-induced uniaxial magnetic anisotropy from negative to positive value continuously thus realize the in-plane SRT in a controlled way.

2. Experiment

A 10 mm × 10 mm Cu(001) single crystal substrate was polished into a ~7° vicinal surface with the atomic steps parallel to the [110] crystalline axis, before transferring it into an ultra high vacuum (UHV) molecular beam epitaxy system with a base pressure of 5.5×10^{-10} Torr. Before the sample growth, the substrate was sputtered by Ar ion at 2–5 keV and annealed at 600 °C for several cycles until split spots were observed in Low Energy Electron Diffraction (LEED) [Fig. 1(b)]. These sharp split spots in Fig. 1(b) indicate the formation of high quality vicinal Cu(001) surface. Py and Co films were expitaxially grown into cross wedges [Fig. 1(a)] by moving the substrate behind a knife-edge shutter during the film growth. As it is shown in the literature, the double wedged sample facilitates a systematic study as a function of film thickness. Finally, a 3 nm Cu film was grown on top of the Co/Py bilayer film to prevent the sample from contamination. The epitaxial growth nature of the vicinal Cu/Co/Py/Cu(001) was testified by the LEED patterns [Fig. 1(b)]. In particular, the split double LEED spots in both the Py and Co films show that the aligned atomic steps on the Cu(001) surface are carried over to the Py and Co overlayers. After the sample growth, in-situ Magneto-Optic Kerr Effect (MOKE) measurements were performed to obtain the magnetic hysteresis loop of the sample. Then the sample was taken out of the UHV chamber and measured by a table top rotation MOKE (ROTMOKE) setup to analyze the magnetic anisotropy quantitatively. All MOKE and ROTMOKE measurements were carried out at room temperature.

3. Results and discussion

We first present hysteresis loops of Cu/Co/Py/vicinal Cu(001) at different film thicknesses. We do not observe hysteresis loops for magnetic field applied perpendicular to the film plane in the thickness range studied, showing that the magnetization is always in the film plane. Therefore we only present the in-plane magnetic hysteresis loops in this paper. At zero Co thickness ($d_{Co}=0$ ML), the hysteresis loop exhibits an easy-axis character with a full remanence for magnetic field applied perpendicular to the atomic steps, and a hard-axis character with small remanence for magnetic field applied parallel to the atomic steps (Fig. 2). This result shows that the atomic steps on the Cu(001) vicinal surface induces an in-plane uniaxial magnetic anisotropy in the vicinal Cu/Py/Cu (001) film with the easy magnetization axis perpendicular to the atomic steps. With increasing the Co thickness, the hard axis loop for field parallel to the atomic steps changes gradually to an easy axis loop with a full remanence. Meanwhile the easy axis loop for field perpendicular to the steps changes gradually to a hard axis loop. This result shows that the addition of the Co layer on top of Py changes the easy magnetization axis from perpendicular to parallel direction of the atomic steps, i.e., there exists an in-plane 90° SRT with increasing the Co thickness. In addition, the steps in the hard axis loop at thicker Co films resemble the hard axis loop in vicinal Co/Cu(001) system [33], indicating the important role of the Co in the SRT and the existence of a 4-fold magnetic anisotropy in vicinal Cu/Co/Py/Cu(001). Qualitatively, it is not surprising to observe the in-plane SRT because of the orthogonal easy axes in vicinal Py/Cu(001) and vicinal Co/Cu(001) systems. However, to understand this SRT quantitatively, we need a systematic study as a function of the Co thickness in vicinal Co/Py/Cu(001).

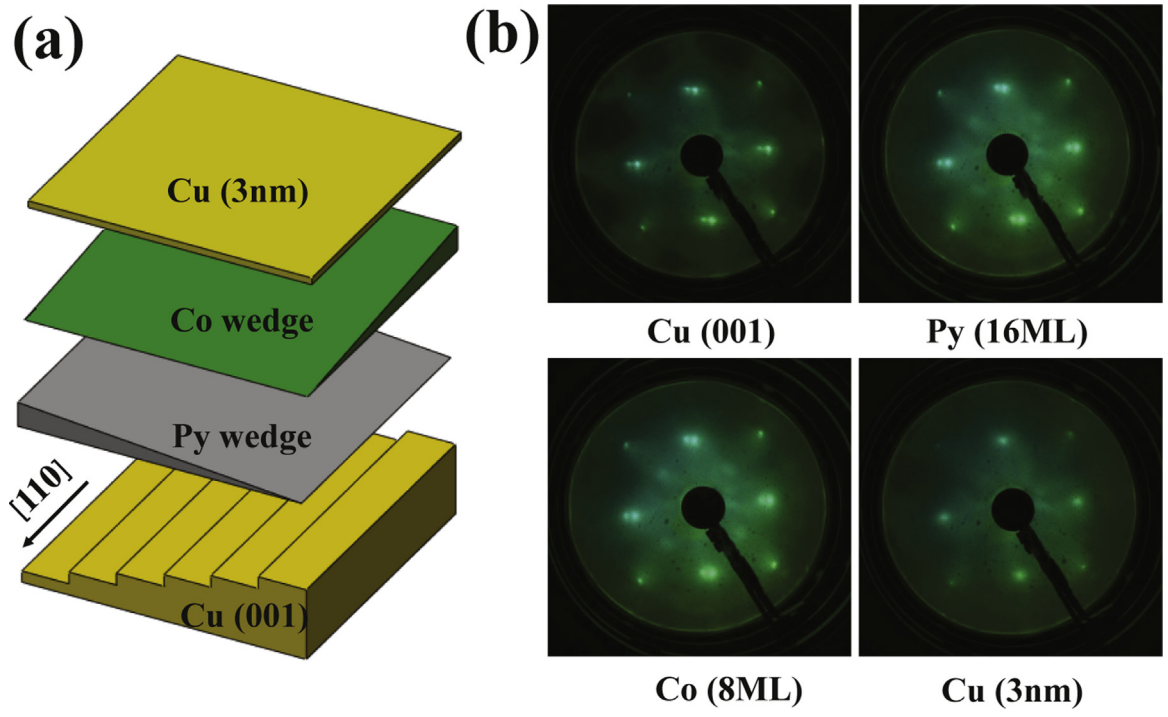

Fig. 1. (a) Schematic drawing of the double wedged Co/Py films grown on vicinal Cu(001). (b) LEED patterns taken at E ~ 130 eV at each growth stage of the vicinal Cu/Co/Py/Cu(001).

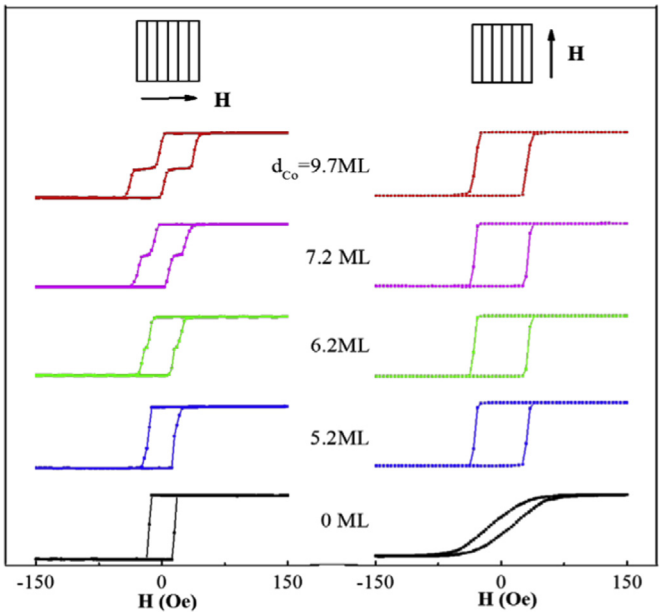

Fig. 2. In-plane hysteresis loops of vicinal Cu/Co/Py(15.5 ML)/Cu(001) for magnetic field applied perpendicular (left column) and parallel (right column) to the atomic steps. An in-plane SRT occurs with increasing the Co film thickness.

ROTMOKE has been proven to be a very effective and well defined technique to measure the in-plane magnetic anisotropy constant [34,35], and thus we applied this method to determine the magnetic anisotropy of vicinal Cu/Co/Py/Cu(001) as a function of Py and Co film thicknesses. Fig. 3(a) shows the schematic drawing of our ROTMOKE experiment. The laser incident optical plane is set to be perpendicular to the atomic steps (the Py in-plane easy magnetization axis) so that the ROTMOKE measures the projection of the magnetization on the Py easy axis [e.g., $\cos(\varphi_M)$, where φ_M is the angle between the magnetization and the Py easy axis]. As the applied magnetic field rotates in the film plane, the magnetic anisotropy deviates the magnetization direction away from the magnetic field direction (φ_H) so that the angular difference between the magnetization and the magnetic field contains the information of the magnetic anisotropy. Therefore an experimental determination of $\cos(\varphi_M)$ as a function of φ_H will derive the magnetic anisotropy of the film. Moreover, the quadratic effect is removed from our experimental results by combining measurements of rotating applied magnetic field cw and ccw.

In order to understand the influence of Co overlayer on the magnetic anisotropy of vicinal Py/Cu(001) films, or this SRT, we need to know the magnetic anisotropy of vicinal Py/Cu(001) films themselves. Therefore, the ROTMOKE measurement was implemented on vicinal Cu/Py/Cu(001) films. The magnetic energy per unit area of the Py film within a magnetic field can be expressed as

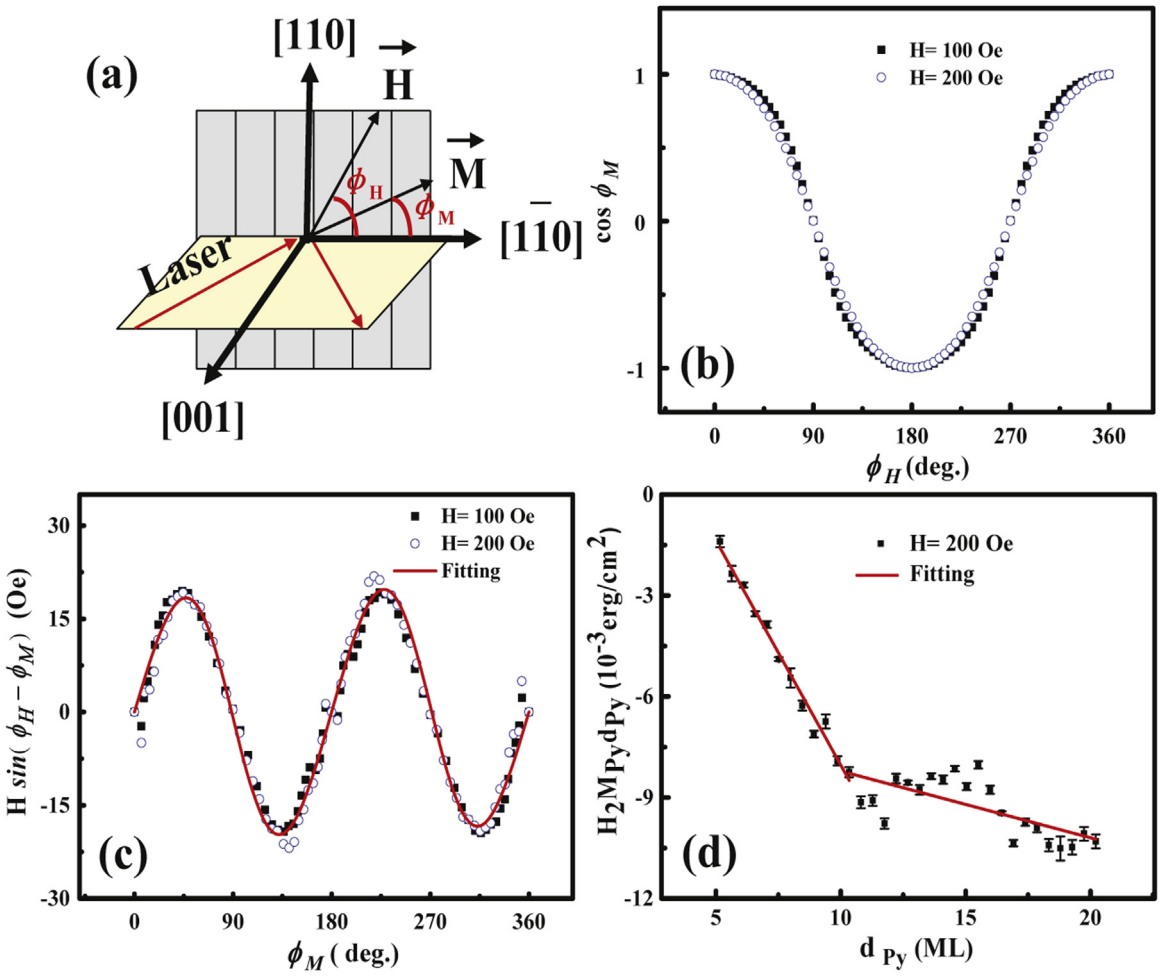

Fig. 3. (a) Schematic drawing of the ROTMOKE experimental condition. (b) The projection ($\cos\ \varphi_M$) of the magnetization from vicinal Cu/Py(6.6 ML)/Cu(001) on the [1$\bar{1}$0] direction as a function of φ_H at magnetic field of 100 Oe and 200 Oe, respectively. (c) Magnetic torque of $H\ \sin(\varphi_H - \varphi_M)$ as a function of φ_M. The red line is the fitting result using eqn. (2). (d) The anisotropy field versus Py thickness. A linear fit using eqn. (3) determines the surface and volume parts of the step-induced uniaxial magnetic anisotropy in the $d_{Py} < 10$ ML and $d_{Py} > 10$ ML regions.

$$E = -M_{Py}d_{Py}H\cos(\varphi_H-\varphi_M)+(2K^S_{2,Py/Cu}+K^V_{2,Py}d_{Py})\cos^2\varphi_M \quad (1)$$

The Py 4-fold anisotropy has been neglected because of its extremely tiny value. $K^S_{2,Py/Cu}$ and $K^V_{2,Py}$ are the step-induced uniaxial magnetic anisotropy contributed from the Py/Cu interface and the Py volume, respectively. The factor of 2 in front of $K^S_{2,Py/Cu}$ specifies the two Py/Cu interfaces of a single Py film. A negative value of K_2 favors an easy magnetization axis perpendicular to the atomic steps. Minimizing Eq. (1) with respect to φ_M yields the magnetic torque equilibrium equation.

$$H\sin(\varphi_H-\varphi_M) = -\frac{H_2}{2}\sin(2\varphi_M) \quad (2)$$

$$H_2M_{Py}d_{Py} = 4K^S_{2,Py/Cu}+2K^V_{2,Py}d_{Py} \quad (3)$$

Since φ_H is given by the magnetic field direction and $\cos\varphi_M$ is determined by the ROTMOKE measurement, the magnetic torque $H\sin(\varphi_H-\varphi_M)$ can be constructed as a function of φ_M from the ROTMOKE measurement. Obviously, the magnetic field strength in ROTMOKE needs to be strong enough to align the magnetization into a single domain but weak enough to permit an appreciable difference between φ_M and φ_H. Fig. 3(b) shows the $\cos(\varphi_M)$ value from ROTMOKE measurement for $d_{Py}=6.6$ ML film as a function of φ_H using a magnetic field of 100 Oe and 200 Oe, respectively. Even as the $\cos(\varphi_M)$ values at these two magnetic field strengths are different, the magnetic torques of $H\sin(\varphi_H-\varphi_M)$ at these two fields are almost identical [Fig. 3(c)], justifying the principle of ROTMOKE technique. Therefore $H=200$ Oe is chosen as the ROTMOKE magnetic field for all films in this work. Then we use Eq. (2) to fit the experimental data [red line in Fig. 3(c)], yielding the anisotropy field of H_2 which determines the overall uniaxial anisotropy $H_2M_{Py}d_{Py}=4K^S_{2,Py/Cu}+2K^V_{2,Py}d_{Py}$. Repeating the ROTMOKE measurement at different Py thicknesses along the Py wedge then allows the separation of the interfacial and volume anisotropies. Fig. 3(d) shows result of $H_2M_{Py}d_{Py}$ as a function of d_{Py}, where $M_{Py}=800$ Oe and 1.77 Å/ML have been adopted for Py in calculation. The result displays that the Py magnetic anisotropy depends linearly on the Py thickness as described by Eq. (3) but with different slopes below and above 10 ML thickness. A linear fitting using eqn. (3) yields $K^S_{2,Py/Cu}=(1.3\pm0.1)\times10^{-3}$ erg/cm^2 and $K^V_{2,Py}=-(3.77\pm0.15)\times10^4$ erg/cm^3 for $d_{Py}<10$ ML; and $K^S_{2,Py/Cu}=-(1.5\pm0.2)\times10^{-3}$ erg/cm^2 and $K^V_{2,Py}=-(5.59\pm0.13)\times10^3$ erg/cm^3 for $d_{Py}>10$ ML. The different magnetic anisotropies below and above 10 ML thickness indicate that the Py film undergoes some intrinsic changes across 10 ML thickness. Hashim et al. [36] show that a Py film grown on Cu(10–50 nm)/Si(001) undergoes a strain relaxation above a critical thickness of ~4.1 nm. However, the change of the lattice constant is too small to be determined by Reflection High Energy Electron Diffraction measurement. The surface lattice constant only shows fluctuations around the Py lattice constant above 2 nm. On the other hand, theoretical calculation shows that even a lattice constant change as tiny as 0.01Å in Ni/Cu(001) could give rise to an anisotropy change of 20 μeV/atom which corresponds to a change of 6×10^{-2} erg/cm^2 for surface anisotropy or a change of 3×10^6 erg/cm^3 for volume anisotropy [37]. Therefore we speculate that the different anisotropies below and above 10 ML in our experiment are due to the different Py strains in these two regions even though a determination of the lattice constant difference is beyond current experimental sensitivity.

After obtaining the step-induced magnetic anisotropy in vicinal Cu/Py/Cu(001), we investigated the SRT in vicinal Cu/Co/Py/Cu (001) by performing ROTMOKE measurement as a function of Co film thickness. Considering the different Py magnetic anisotropies below and above 10 ML thickness, we chose two different Py thicknesses of $d_{Py}=7.2$ ML and $d_{Py}=15.5$ ML for the SRT study. Taking the fact that the Co and Py magnetizations are coupled rigidly together, the magnetic anisotropy energy per unit area for a Co/Py bilayer film should be

$$\begin{aligned}E = &-(M_{Py}d_{Py}+M_{Co}d_{Co})H\cos(\varphi_H-\varphi_M)\\ &+(K^S_{2,Py/Cu}+K^S_{2,Cu/Co/Py}+K^V_{2,Py}d_{Py}+K^V_{2,Co}d_{Co})\cos^2\varphi_M\\ &+(K^S_{4,Cu/Co/Py}+K^V_{4,Co}d_{Co})\cos^2\left(\varphi_M-\frac{\pi}{4}\right)\sin^2\left(\varphi_M-\frac{\pi}{4}\right)\end{aligned} \quad (4)$$

Here $K^S_{Cu/Co/Py}$ includes both the Py/Co and the Co/Cu interfacial anisotropies, and K^V denote the volume anisotropy with the subscription specifying the film. The subscriptions of "2" and "4" stand for the uniaxial and 4-fold anisotropies, respectively. The 4-fold anisotropy of Py film is still ignored as mentioned before. Minimizing Eq. (4) yields the following equation.

$$H\sin(\varphi_H-\varphi_M) = -\frac{H_2}{2}\sin(2\varphi_M)-\frac{H_4}{4}\sin(4\varphi_M) \quad (5)$$

with

$$\begin{aligned}H_2(M_{Py}d_{Py}+M_{Co}d_{Co}) = &\,2K^S_{2,Py/Cu}+2K^S_{2,Cu/Co/Py}+2K^V_{2,Py}d_{Py}\\ &+2K^V_{2,Co}d_{Co}C\end{aligned} \quad (6)$$

$$H_4(M_{Py}d_{Py}+M_{Co}d_{Co}) = 2K^S_{4,Cu/Co/Py}+2K^V_{4,Co}d_{Co} \quad (7)$$

Fitting the magnetic torque using Eq. (5) extracts the H_2 and H_4 for the bilayer films [Fig. 4(a)], respectively. It is seen that both H_2 and H_4 change monotonically with increasing the Co thickness, showing that the anisotropies of the Py/Co bilayers evolve with increasing the Co layer thickness. The most important observation is that there is a crossover of H_2 from negative to positive values as the Co thickness increases, demonstrating the existence of an in-plane SRT of the easy magnetization axis from perpendicular to parallel directions of the atomic steps from the viewpoint of quantitative analysis. The $H_2=0$ point occurs at $d_{Co}\sim3$ ML for $d_{Py}=7.2$ ML, and at $d_{Co}\sim4$ ML for $d_{Py}=15.5$ ML. The thicker Co critical thickness in $d_{Py}=15.5$ ML film than in $d_{Py}=7.2$ ML is expected because the Co layer needs to overcome a stronger uniaxial anisotropy for thicker Py film. We can further single out the Co anisotropy constants using Eqs. (6) and (7). Since Py film has different magnetic anisotropy constants below and above 10 ML, we need to use different values of $K^S_{2,Py/Cu}$ and $K^V_{2,Py}$ when applying Eq. (6) to the $d_{Py}=7.2$ ML and $d_{Py}=15.5$ ML bilayer films. As shown in Fig. 4(b), the two data sets in both the $H_2(M_{Py}d_{Py}+M_{Co}d_{Co})-2K^V_{2,Py}d_{Py}-2K^S_{2,Py/Cu}$ and the $H_4(M_{Py}d_{Py}+M_{Co}d_{Co})$ collapse into a universal straight line. Then the slope and the intersection of the straight line at $d_{Co}=0$ should correspond to the Co volume and surface (the two Py/Co/Cu interfaces) anisotropies. By a linear fitting [the red line in Fig. 4(b)], we derive that $K^S_{2,Cu/Co/Py}=-(7.0\pm0.6)\times10^{-3}$ erg/cm^2, $K^V_{2,Co}=(1.74\pm0.06)\times10^5$ erg/cm^3, $K^S_{4,Cu/Co/Py}=(4.0\pm0.2)\times10^{-2}$ erg/cm^2, and $K^V_{4,Co}=-(7.9\pm0.2)\times10^5$ erg/cm^3. Considering the interface anisotropy changes with the thickness, we should fit the uniaxial anisotropy of Co film independently for these two different Py film thickness. By doing so we found that there is negligible difference in the Co volume and interface anisotropies with Py thickness. The deviation of the 4-fold volume anisotropy data points from the straight line below 3 ML Co could be attributed to the fact that the volume anisotropy should be better defined only when the 3-dimensional lattice structure is established above 3 ML thickness.

From the ROTMOKE results, the uniaxial magnetic anisotropy is contributed from both the surface and volume anisotropies. On the other hand, a uniaxial anisotropy does not exist in a (001) film because of the 4-fold rotation symmetry. Therefore although manifested as the surface and volume anisotropies, the uniaxial anisotropy must be originated from the atomic steps on the vicinal

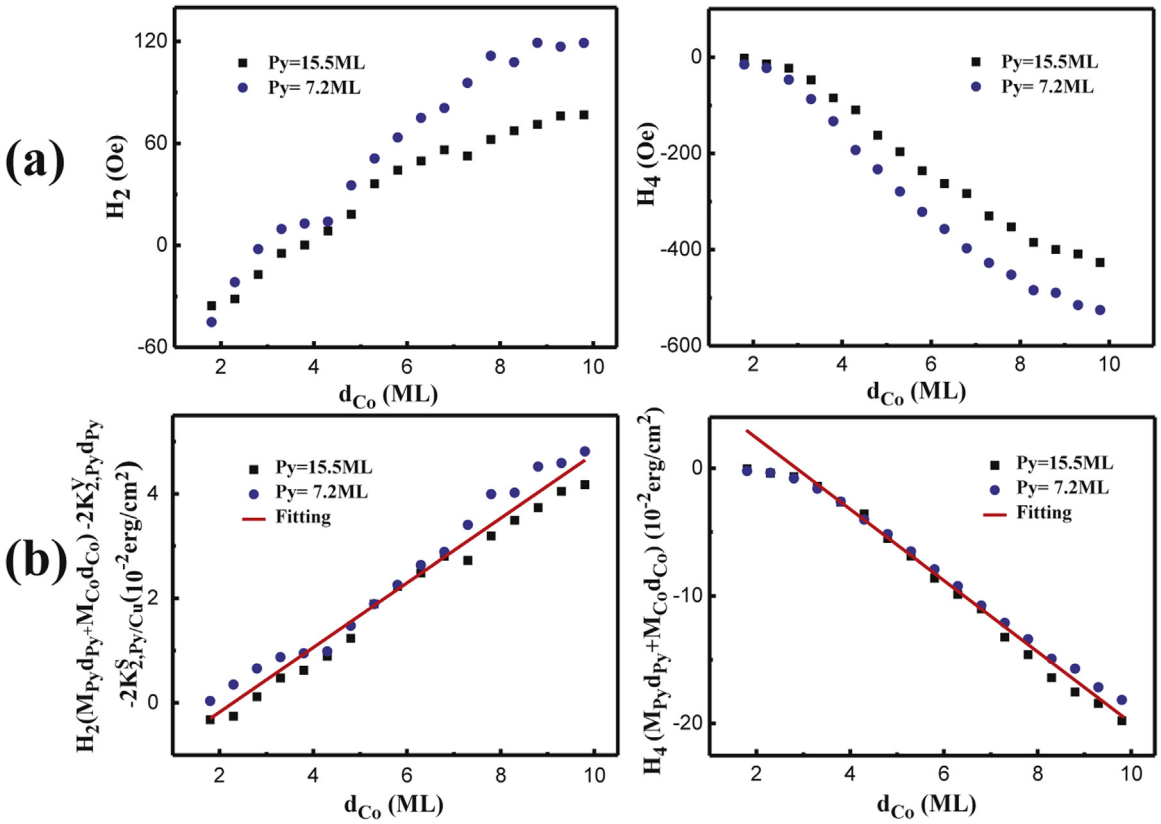

Fig. 4. (a) Magnetic anisotropy fields of H_2 and H_4 versus Co thickness for vicinal Cu/Co/Py/Cu(001) at $d_{Py}=7.2$ ML and $d_{Py}=15.5$ ML. (b) $H_2(M_{Py}d_{Py}+M_{Co}d_{Co})-2K^V_{2,Py}d_{Py}-2K^S_{2,Py/Cu}$ and $H_4(M_{Py}d_{Py}+M_{Co}d_{Co})$ versus Co thickness. The collapse of the two curves in (a) into a straight line shows the validity of Eqs. (6) and (7). (For interpretation of the references to color in this figure, the reader is referred to the web version of this article.)

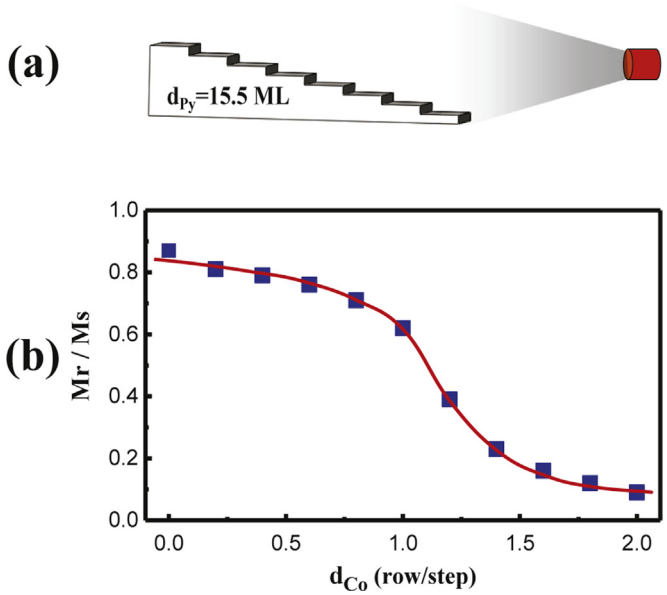

Fig. 5. (a) Schematic drawing of the side-growth geometry. (b) Magnetic remanence as a function of the side-growth Co thickness for magnetic field perpendicular to the steps.

surface. This fact implies that a modulation of the step edges should be more effective to change the uniaxial magnetic anisotropy than a modulation away from the step edges. In fact, it was shown that Cu atoms on a stepped Co film tend to migrate to the Co step edges at room temperature and subsequently only a fraction of one monolayer Cu can modulate significantly the uniaxial magnetic anisotropy [33]. However, we did not observe the same phenomenon in the vicinal Cu/Co/Py/Cu(001) system, i.e., the uniaxial anisotropy of the Py film does not change significantly in the submonolayer regime of the Co overlayer. This is probably due to the low mobility of Co atoms on Py surface so that Co ascorbate atoms stay where they land on the Py surface at room temperature. To verify the fact that Co absorption at the Py step edges should modulate significantly the uniaxial magnetic anisotropy, we grew a Co film wedge (0–2 ML) on a stepped Py film (15.5 ML) at room temperature by side-growth geometry as shown in Fig. 5(a). It was shown that the side growth promotes the adatoms to reach the step edges of a vicinal surface and a full row of Co decoration at one step edge is accomplished when the deposition time corresponds to an equivalent 1 ML Co in the [110] direction. Fig. 5(b) shows the magnetic remanence (normalized by the saturation magnetization) from MOKE hysteresis loop measurement as a function of the side-growth Co thickness for magnetic field applied along the Py easy magnetization axis. The magnetic remanence drops drastically in the range of 1.0 row/step $< d_{Co} <$ 1.4 row/step. Note that 1 row/step Co is equivalent to only 0.12 ML in the normal growth, the SRT at $\sim$1 row/step in Fig. 5(b) indicates that step-induced uniaxial anisotropy indeed originates from the step edges.

4. Summary

In conclusion, we investigated vicinal Cu/Co/Py/Cu(001) with the atomic steps parallel to the [110] crystal axis. The atomic steps induce a uniaxial magnetic anisotropy in Cu/Py/Cu(001) film with the easy magnetization axis perpendicular to the atomic steps. The addition of Co overlayer generates an in-plane spin reorientation transition of the vicinal Cu/Co/Py/Cu(001) films from perpendicular

to parallel direction of the atomic steps. Using ROTMOKE measurement, we determined systematically the uniaxial and 4-fold magnetic anisotropies and explain that the SRT occurs as a result of the opposite signs of the step-induced uniaxial magnetic anisotropy in Py and Co films, respectively. Furthermore, step decoration by side-growth shows that the uniaxial magnetic anisotropy indeed originates from the step edges.

Acknowledgment

Financial support through National Science Foundation DMR-1504568 NRF through the Global Research Laboratory project of Korea is gratefully acknowledged. J.D. acknowledges fellowship support from the China Scholarship Council and National Natural Science Foundation of China under Grant no. 51331006.

References

[1] U. Gradmann, J. Korecki, G. Waller, Appl. Phys. A 39 (1986) 101.
[2] D. Wang, R. Wu, A.J. Freeman, Phys. Rev. Lett. 70 (1993) 869.
[3] C.A.F. Vaz, J.A.C. Bland, G. Lauhoff, Rep. Prog. Phys. 71 (2008) 056501.
[4] M.T. Johnson, P.J.H. Bloemen, F.J.A. den Broeder, J.J. de Vries, Rep. Prog. Phys. 59 (1996) 1409.
[5] D.P. Pappas, K.-P. Kämper, H. Hopster, Phys. Rev. Lett. 64 (1990) 3179.
[6] Z.Q. Qiu, J. Pearson, S.D. Bader, Phys. Rev. Lett. 70 (1993) 1006.
[7] Wupeng Cai, Shiji Muraishi, Ji Shi, Yoshio Nakamura, Wei Liu, Ronghai Yu, Appl. Phys. A 109 (2012) 69.
[8] D.P. Pappas, C.R. Brundle, H. Hopster, Phys. Rev. B 45 (1992) 8169.
[9] J.A.C. Bland, G.A. Gehring, B. Kaplan, C. Daboo, J. Magn. Magn. Mater. 113 (1992) 173.
[10] D. Wilgocka-Ślęzak, K. Freindl, A. Kozioł, K. Matlak, M. Rams, N. Spiridis, M. Ślęzak, T. Ślęzak, M. Zając, J. Korecki, Phys. Rev. B 81 (2010) 064421.
[11] B.F. Miao, Y.T. Millev, L. Sun, B. You, W. Zhang, H.F. Ding, Sci. China Phys. Mech. Astron. 56 (2013) 70.
[12] K. Baberschke, M. Farle, J. Appl. Phys. 81 (1997) 5038.
[13] Ying-Ta Shih, Wen-He Shen, Kuo-Long Lee, Wei Pan, AIP Adv. 4 (2014) 017132.
[14] W.C. Minn-Tsong Lin, C.C. Lin, Kuo, C.L. Chiu, Phys. Rev. B 62 (2000) 14268.
[15] R. Allenspach, A. Bischof, Phys. Rev. Lett. 69 (1992) 3385.
[16] O. Portmann, A. Vaterlaus, D. Pescia, Nature 422 (2003) 701.
[17] Y.Z. Wu, C. Won, A. Scholl, A. Doran, H.W. Zhao, X.F. Jin, Z.Q. Qiu, Phys. Rev. Lett. 93 (2004) 117205.
[18] J. Choi, J. Wu, C. Won, Y.Z. Wu, A. Scholl, A. Doran, T. Owens, Z.Q. Qiu, Phys. Rev. Lett. 98 (2007) 207205.
[19] R. Lavrijsen, D.M.F. Hartmann, A. van den Brink, Y. Yin, B. Barcones, R.A. Duine, M.A. Verheijen, H.J.M. Swagten, B. Koopmans, Phys. Rev. B 91 (2015) 104414.
[20] A. Berger, U. Linke, H.P. Oepen, Phys. Rev. Lett. 68 (1992) 839.
[21] M.N. Wilson, A.B. Butenko, A.N. Bogdanov, T.L. Monchesky, Phys. Rev. B 89 (2014) 094411.
[22] M.V. Sapozhnikov, O.L. Ermolaeva, Phys. Rev. B 91 (2015) 024418.
[23] J. Chen, J.L. Erskine, Phys. Rev. Lett. 68 (1992) 1212.
[24] W. Weber, C.H. Back, A. Bischof, Ch Würsch, R. Allenspach, Phys. Rev. Lett. 76 (1996) 1940.
[25] Yongsup Park, Eric E. Fullerton, S.D. Bader, Appl. Phys. Lett. 66 (1995) 2140.
[26] J.H. Wolfe, R.K. Kawakami, W.L. Ling, Z.Q. Qiu, Rodrigo Arias, D.L. Mills, J. Magn. Magn. Mater. 232 (2001) 36.
[27] S. Finizio, M. Foerster, M. Buzzi, B. Krüger, M. Jourdan, C.A.F. Vaz, J. Hockel, T. Miyawaki, A. Tkach, S. Valencia, F. Kronast, G.P. Carman, F. Nolting, M. Kläui, Phys. Rev. Appl. 1 (2014) 021001.
[28] R. Höllinger, M. Zölfl, R. Moosbühler, G. Bayreuther, J. Appl. Phys. 89 (2001) 7136.
[29] J. Li, M. Przybylski, F. Yildiz, X.L. Fu, Y.Z. Wu, Phys. Rev. B 83 (2011) 094436.
[30] U. Welp, V.K. Vlasko-Vlasov, Phys. Rev. Lett. 90 (2003) 167206.
[31] Q. Li, T. Gu, J. Zhu, Z. Ding, J.X. Li, J.H. Liang, Y.M. Luo, Z. Hu, C.Y. Hua, H.-J. Lin, T. W. Pi, C. Won, Y.Z. Wu, Phys. Rev. B 91 (2015) 104424.
[32] S. Ma, A. Tan, J.X. Deng, J. Li, Z.D. Zhang, C. Hwang, Z.Q. Qiu, Sci. Rep. 5 (2015) 11055.
[33] R.K. Kawakami, M.O. Bowen, Hyuk J. Choi, Ernesto J. Escorcia-Aparicio, Z. Q. Qiu, Phys. Rev. B 58 (1998) R5924.
[34] R. Mattheis, G. Quednau, J. Magn. Magn. Mater. 205 (1999) 143.
[35] Z. Tian, C.S. Tian, L.F. Yin, D. Wu, G.S. Dong, X.F. Jin, Z.Q. Qiu, Phys. Rev. B 70 (2004) 012301.
[36] I. Hashim, H.A. Atwater, J. Appl. Phys. 75 (1994) 6516.
[37] O. Hjortstam, K. Baberschke, J.M. Wills, B. Johansson, O. Eriksson, Phys. Rev. B 55 (1997) 15026.